Available online at www.sciencedirect.com
SCIENCE DIRECT®
Analytica Chimica Acta 479 (2003) 151–165
ANALYTICA CHIMICA ACTA
www.elsevier.com/locate/aca

Portable flow-injection analyzer with liquid-core waveguide based fluorescence, luminescence, and long path length absorbance detector

Qingyang Li [a], Kavin J. Morris [a], Purnendu K. Dasgupta [a,*], Ivo M. Raimundo Jr. [b], Henryk Temkin [c]

[a] *Department of Chemistry and Biochemistry, Texas Tech University, Box 41061, Lubbock, TX 79409-1061, USA*
[b] *Instituto Quimica, Universidade Estadual Campinas, Instituto Quimica, Campinas, SP, Brazil*
[c] *Jack Maddox Laboratory, Department of Electrical Engineering, Texas Tech University, Lubbock, TX 79409-3102, USA*

Received 8 October 2002; received in revised form 25 November 2002; accepted 27 November 2002

Abstract

We describe a multifunctional flow analysis instrument that is portable (25 cm × 20 cm × 11 cm, 2.3 kg) for facile field deployment. Using a 50 cm long Teflon® AF tubing as final reaction and optical measurement conduit, we combine a liquid-core waveguide (LCW) based fluorescence detector that is transversely illuminated by an addressable light emitting diode array, a chemiluminescence (CL) detector and an absorbance detector with a solid-state broadband (400–700 nm) source. Several illustrative experiments have been carried out to test the performance of the instrument in different detection modes. A S/N = 3 limit of detection (LOD) of 0.25 $\mu g\,l^{-1}$ for chromium(VI) was established using the diphenylcarbazide chemistry, and an LOD of 5 $\mu g\,l^{-1}$ was similarly established for Al(III), using Pyrocatechol Violet (PCV) as the chelating chromogenic dye, in both cases using long path absorption detection. The LOD for aqueous hydrogen peroxide was 16 nM using a fluorescence method based on the formation of thiochrome from thiamine and 4 nM by a luminol chemiluminescence method. With a Nafion membrane diffusion scrubber (DS), the LOD was 8.0 pptv for gaseous hydrogen peroxide by the fluorescence method.

Keywords: Liquid-core waveguide; Long path length absorbance; Hydrogen peroxide; Multipurpose LED-based absorbance/fluorescence detector

1. Introduction

Field-portable methods of analysis are becoming increasingly important. While the possibilities once available to an analytical chemist merely consisted of test kits, presently many sophisticated instruments are becoming available for portable use in a convenient form. Solution phase optical methods, notably chemistries that involve absorbance and fluorescence measurements constitute by far the largest segment of analytical methods in use today. For the automation of solution phase analytical methods, flow-injection analysis was introduced by Ruzicka and Hansen [1] and sequential injection analysis techniques were introduced by Ruzicka and Marshall [2].

Among optical detection methods, fluorescence and chemiluminescence (CL) methods are known to be particularly sensitive, however, these methods are

* Corresponding author. Tel.: +1-8067423067; fax: +1-8067421289.
E-mail address: sandy.dasgupta@ttu.edu (P.K. Dasgupta).

0003-2670/03/$ – see front matter
doi:10.1016/S0003-2670(02)01531-3

not as commonly applicable as absorption detection, which is by far the most common quantitation method in analytical chemistry. Absorption of light by an analyte or some product generated therefrom is governed, as is well known, by Beer's law. The limit of detection (LOD) is controlled by the minimum absorbance change that can be detected, which is also a function of the measurement noise. For a given analyte concentration, the measured absorbance is maximized by the proper choice of (chromogenic) chemistry and the choice of the wavelength. This is routinely carried out and considered standard practice. It may seem that it is equally obvious to increase the optical path length since the measured absorbance is linearly related to the path length. In reality, despite focusing optics, light passing through a dense phase such as an aqueous solution diverges rapidly and most of the light in practical flow-cells is rapidly lost to the cell walls. The deterioration of light throughput causes a concomitant increase in noise. Practitioners know that in most cases beyond a fairly modest path length of 6–20 mm, the attainable LOD actually deteriorates with increasing path length ([3,4] and references therein).

The solution to this dilemma has also been known for some time. This is to make the measurement cell behave as an optical fiber or a light guide, such that light undergoes total internal reflection at the walls. In an optical fiber, not only the light-conducting path is transparent in the wavelength range of interest, the core region of the fiber has a refractive index (RI) greater than that of the cladding material such that light remains trapped in the optically denser core. It is only since the advent of Teflon® AF (AF is an acronym for amorphous fluoro polymer), a polymer that is largely transparent throughout the UV and visible range and with a RI of 1.29–1.31 such that a water core light guide (the RI of water is 1.33) has become possible in recent years. It is possible to increase the sensitivity for absorption detection, up to two orders of magnitude, using a light guide cell [5–17].

Further, the unique optical property of Teflon® AF permits a simple and stable transversely illuminated fluorescence detector [18–24]. We have also recently shown a liquid-core waveguide (LCW) chemiluminescence (CL) detector. A high detection sensitivity is attained with inexpensive PMTs, because the LCW can effectively collect and transfer much of the CL emission [18,25,26].

In the present work, we combine a long path length absorption (LPLA) detector, a CL detector and a fluorescence detector with a custom miniature peristaltic pump and thus provide an inexpensive portable FIA instrument and demonstrate that it is widely applicable to a variety of analysis needs permitting high sensitivity.

2. Experimental

2.1. Apparatus

The construction of the LCW based detector is shown in Fig. 1. The Teflon® AF-2400 tube (i.d. 0.56 mm, o.d. 0.80 mm, 500 mm in length, Biogeneral Inc., San Diego, CA) is located in a U-shaped curve on a black opaque acrylic sheet and sealed by another opaque acrylic sheet to protect the AF tube physically and to avoid ambient light. The left end of the Teflon® AF tube butts up against a 1 mm core jacketed acrylic fiber optic through the opposing arms of a purpose-machined opaque tee. The arrangement at both tee ends of the Teflon® AF tube is readily configurable by the user. The precise configuration at the right tee and the selection of the detector at the left tee are made based on what mode the instrument is used.

For CL detection, a Teflon® tube brings in the reagent flow stream through the right tee arm while a small o.d. silica capillary (o.d. 350 μm, i.d. 200 μm) inserted into the AF tube (to about 2 cm) and sealed through the long arm of the tee brings in the carrier stream (Fig. 1a). The AF tube works as both the mixing conduit and the CL detection cell [27]. For other reactions, which require longer reaction time, a separate mixing conduit can precede the LCW cell. The light signal is acquired at the instant that it is generated (save for the transit time of light) and unlike many other arrangements, the initial point of confluence is within the field of view of the detector. Thus, even fast CL reactions are efficiently monitored. The acrylic fiber optic is coupled to a compact inexpensive (∼US$ 400) miniature PMT with its own built-in HV power supply (Hamamatsu H5784). A dual JFET operational amplifier (Texas Instruments TL082) is used both to further amplify/offset the signal and filter the high frequency noise of the signal from PMT. The signal is then acquired at 1 Hz by

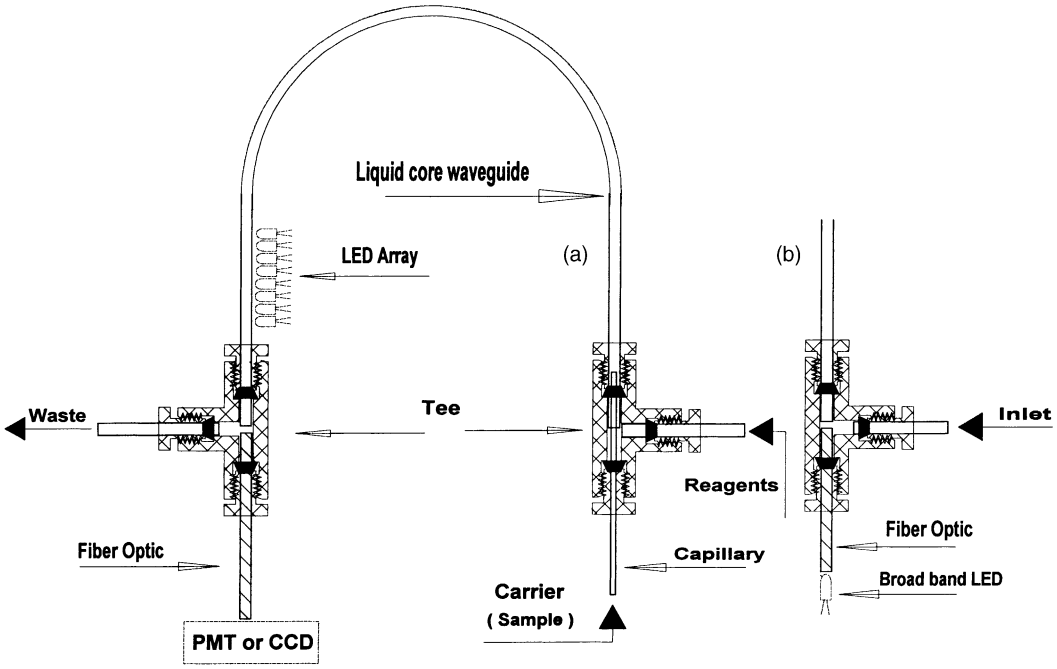

Fig. 1. (a and b) Optical and flow schematic of instrument.

a PCM-DAS16D/12 data acquisition card (Measurement Computing Inc., Middleboro, MA) housed in a mini-notebook personal computer.

For LPLA detection, the detector used at the left tee is a palm-size CCD spectrometer (USB2000, Ocean Optics Inc., Dunedin, FL). Monitoring the signal at a wavelength where the sample does not absorb provides a means of referencing. At the right tee, a white LED (Nichia SPW 500BS) is used as a solid-state broadband light source; it has useful output over the 400–700 nm range. If desired, for dedicated single wavelength measurements, the LED can be readily changed for any other similarly sized (5 mm, T-1 3/4) emitter device. Both the CCD spectrometer and the PMT are accommodated within the main instrument enclosure.

For fluorescence detection, the arrangement of the tees is similar with absorption detection except that the axial (broadband) LED source is turned off and covered with al-foil to eliminate light intrusion, or replaced with a light-tight plug. A homebuilt 12-LED array provides excitation light at selectable wavelengths. The LED array contains 12 different LEDs with different maximum emission wavelengths ranging from 375 to 620 nm, with half bandwidths lying between 12 and 50 nm. The emission spectra of the 12 LEDs are shown in Fig. 2, as read by a photodiode array spectrometer (CDI-PDA-512, Control Development Inc., South Bend, IN; there is some intrinsic bias of these spectrometers towards longer wavelengths). A microcontroller (BASIC Stamp II, Parallax Inc.; Rocklin, CA) receives commands sent from the host PC through the COM port, then interprets the commands and controls a specific LED to turn on or turn off via MOSFET logic switches. All necessary software in this context was written in-house. In dedicated fluorescence detection, only one LED that provides maximum emission light is turned on. However, it is possible to perform a “temporal excitation scan” within the wavelength range provided by the LEDs. This can also be useful in simultaneous multi-analyte detection but was not presently pursued. We have ongoing studies to fabricate AlN/AlGaInN based UV-emitting LED arrays by molecular beam epitaxy techniques [28]. As these devices reach practically useful emission power, this aspect will deserve more

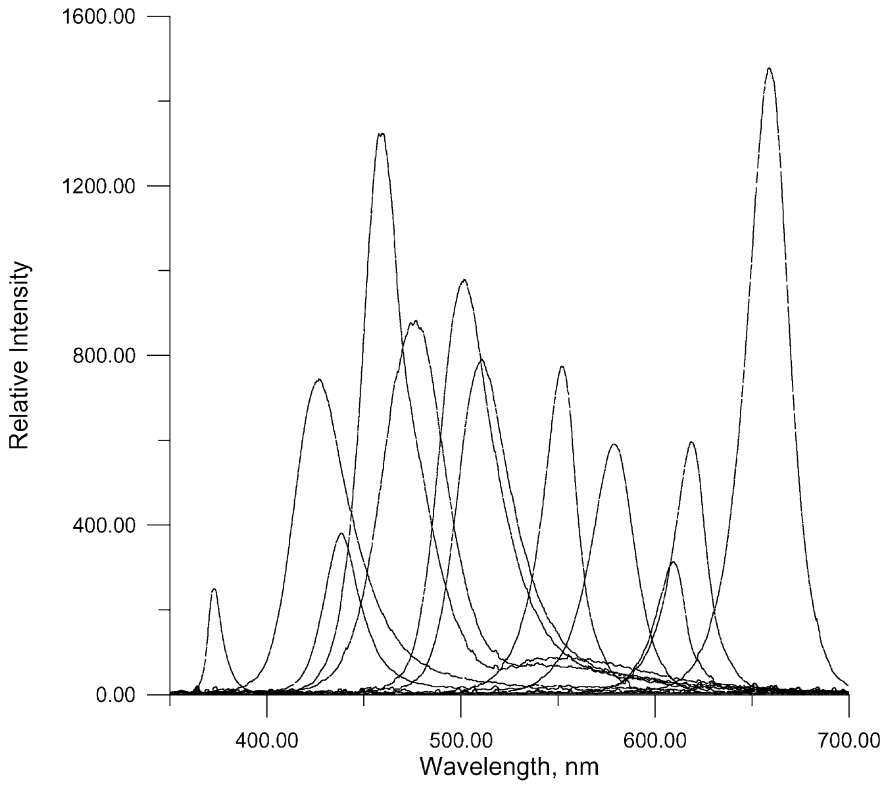

Fig. 2. Spectra for 12 excitation LEDs. The spectra also show the relative intensity of the LEDs as measured by a photodiode array detector. Numbering the LEDs present in the array as 1–12 in order of increasing center wavelength, the intensity is multiplied by a factor of 15 for LED-1, and the intensities of LED-2, LED-8 and LED-9 are multiplied by a factor of 20.

attention. The LED array was put close to the LCW (at a distance <1 mm); the nearest LED to the detector fiber was at a distance of 5 cm. Light from any member of the LED array illuminates the LCW transversely, from the radial direction. Virtually none of the excitation light thus incident orthogonal to the axis of the LCW propagates axially. In contrast, if fluorescence or other elastic or inelastic scattering phenomena occur, any light generated within the LCW that falls within the acceptance cone of the LCW propagates by total internal reflection in both directions and thus the detector sees approximately half of this generated light. This simple arrangement and ready coupling to a receiver fiber without additional optics makes for a very rugged and robust fluorescence detector with excellent sensitivity and little need for monochromators to reject the excitation light from the emitted light. In applications that do not require maximum sensitivity, the CCD spectrometer detector is sufficiently sensitive to serve as the emitted light detector and has the added advantage of providing a fluorescence spectrum. For situations where higher sensitivity is required, the detector fiber is coupled to the PMT and any residual excitation light is removed from the emitted beam by appropriate colored plastic optical filters [29].

Pumping was provided by purpose-machined four-channel miniature peristaltic pump (5.0 cm $\times$ 6.0 cm $\times$ 6.0 cm) driven by a dc gear motor (Jameco Electronics, Belmont, CA, P/N 1555838, 20 rpm at 12 V dc). The rotation speed of the motor can be adjusted by changing the applied voltage. The pump utilized 10 stainless steel rollers with a radial spacing of 8 mm. PVC pumping tubes (Elkay products Inc., MA, USA) with ID of 0.045 in. were used in all the experiments. Samples were injected manually with a six-port loop-type rotary injection

valve (Upchurch, Oak Harbor, WA). Except for the Teflon® AF tube and as otherwise stated, all tubing were PTFE Teflon® (o.d. 1.30 mm, i.d. 0.66 mm). A 20 cm long restriction tube (220 μm i.d.) was added to the system flow exit to inhibit formation of air bubbles in the measurement cell. Four 50-ml bottles to hold solution and waste are integrated in the lid of the instrument. Instrument power is 12 V dc and typically consumes 150 mA (not including the laptop). A socket is provided for connection to external power; an appropriately modified laptop power supply or an external auto/marine battery can provide this power. All necessary parts as described above are contained in the black acrylic instrument enclosure (25 cm × 20 cm × 11 cm, 2.3 kg), except the diffusion scrubber (DS) [30] and ancillary parts needed for gas calibration are not included. The layout of the instrument is shown in Fig. 3 and a photograph is shown in Fig. 4.

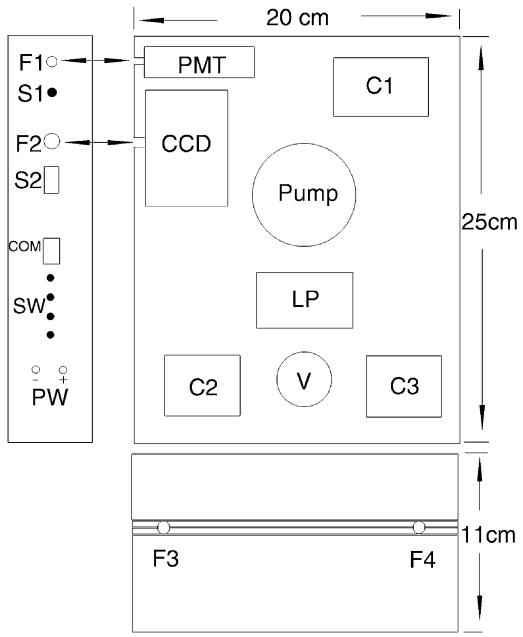

Fig. 3. Layout of the instrument. C1, C2, and C3: electronic circuit boards for PMT, LED array, peristaltic pump, etc.; CCD: CCD spectrometer; COM: male COM port connector to PC; PMT: photomultiplier tube; Pump: peristaltic pump; PW: connectors for power supply; LP: liquid inlet and outlet connector panel; F1: fiber optic connector to photomultiplier tube; F2: fiber optic connector to CCD spectrometer; F3: fiber optic connector to collect signal from Teflon® AF tube, connected to F1 or F2; F4: fiber optic connector for connection to broad band LED source for measurement of absorbance; S1: PMT signal out connector; S2: CCD detector signal out connector; SW: switches for power, pump, PMT and absorption light source.

2.2. Methods and reagents

2.2.1. Long path length absorption (LPLA) determination of chromium(VI) with diphenylcarbazide

In aqueous solution, chromium(VI) oxidizes diphenycarbazide (DPC) to diphenylcarbadiazone, the enol form of which then reacts with the chromium(III) formed to yield a red–purple product (λ_{max}: 540 nm). The reaction has been known for a long time [31] and is part of standard methods [32]. The method is highly selective for Cr(VI) over other metals, and under optimum conditions may provide a detection limit at the sub-nanogram level [33,34].

The flow-injection analysis schematic is shown in Fig. 5. The sample loop (0.66 mm × 600 mm, 200 μl, this loop is used all LPLA experiments and a 240 mm, 80 μl loop is used in fluorescence and CL experiments) is longer than typical FIA practice, because more solution is needed to fill the long-path cell. The DPC reagent was made by adding 7.5 ml 1% (w/v) DPC in acetone, 7.5 ml concentration H_3PO_4 and 35 ml 0.1 M Na_2HPO_4 (final pH ∼1) together. The reagent was pumped at 0.4 ml min^{-1} and merged with the carrier stream (0.4 ml min^{-1}) and mixed in a PTFE mixing conduit (0.66 mm × 6000 mm) that provides a reaction time of 2.5 min prior to detection. Chromium(VI) solution was prepared by dissolving $K_2Cr_2O_7$ in water. The absorbance was detected at 540 nm. The signal at 680 nm was used as the reference.

2.2.2. LPLA determination of aluminum in water with Pyrocatechol Violet (PCV)

Pyrocatechol Violet (PCV) was first introduced by Anton [35] as a chromogenic reagent for the determination of aluminum. The flow-injection manifold is shown in Fig. 6. The PCV solution (0.1 mM) and carrier are prepared in a 0.1 M 2[*N*-morpholino] ethanesulfonic acid (MES, Sigma) buffer solution. Iron can interfere in this reaction and must be masked. The iron-masking solution is 50 mM ascorbic acid [36]. All the solutions are pumped at 0.8 ml min^{-1}. The absorbance was detected at 585 nm and the reference wavelength used was 700 nm.

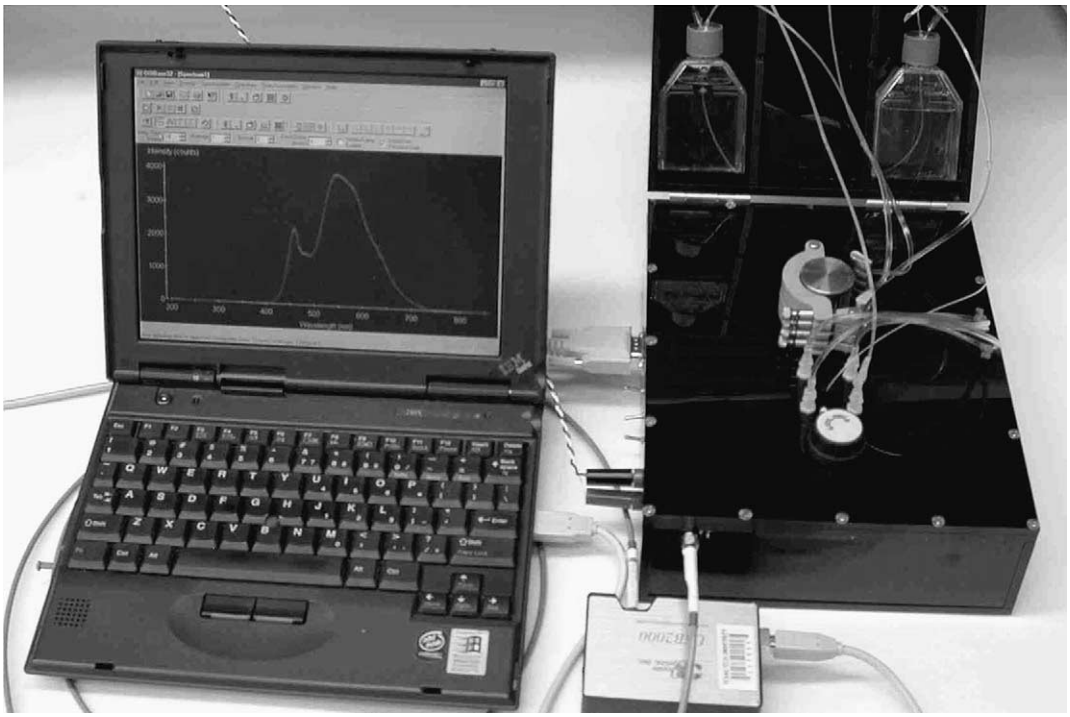

Fig. 4. Photograph of complete instrument. CCD spectrometer placed outside for photo.

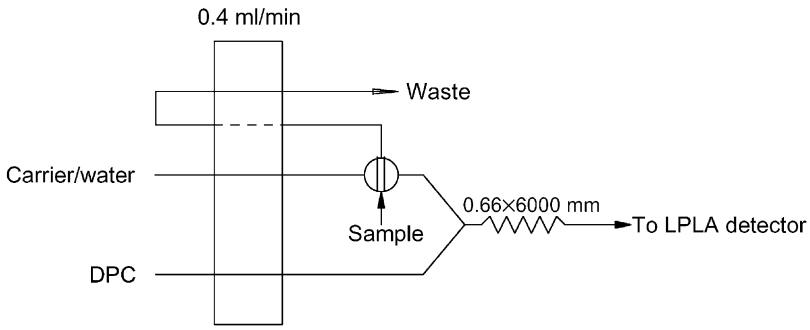

Fig. 5. Flow-injection manifold for the determination of chromium(VI).

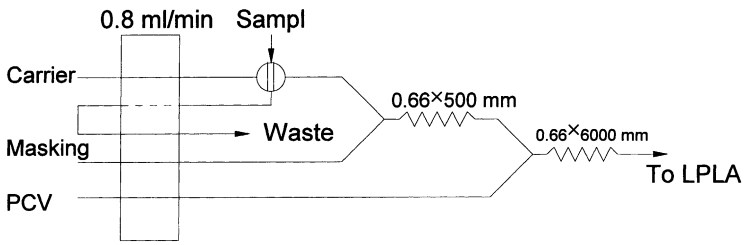

Fig. 6. Flow-injection manifold for determination of aluminum.

2.2.3. Determination of H_2O_2 in gas- and aqueous-phase by fluorometry

The determination principle and instrument schematic is similar to a method already reported in [21]. The chemistry is based on oxidation of nonfluorescent thiamine to fluorescent thiochrome with hematin as a catalyst by hydrogen peroxide. Hematin (10 μM) solution is pumped at 0.14 ml min^{-1} and is merged with the carrier (water) stream (0.14 ml min^{-1}). After a mixing conduit (0.66 mm × 500 mm), the mixed stream reacts with thiamine solution (100 μM thiamine, 5 mM K_2HPO_4, adjusted to pH 12.0 with 2 M NaOH) in another reaction coil (0.66 mm × 3000 mm) and then flows through the LCW based fluorescence detector. A narrow-band (half-width 12 nm) InGaN LED (NSHU 590E, Nichia America Corp.) with its emission centered at 375 nm in the 12-LED array works as excitation light source (LED-1, Fig. 2). A colored plastic filter (No. 861, Edmund Scientific, Barrington, NJ) with a transmittance window centered near the emission maximum of thiochrome is put in front of the PMT to reject residual excitation light. To determine hydrogen peroxide in gas phase, a diffusion scrubber transfers the gas to the liquid phase and the rest of the analytical protocol is the same [21].

2.2.4. Determination of H_2O_2 by luminol chemiluminescence

Chemiluminescence detection capabilities were tested by adapting another reported measurement method for hydrogen peroxide that involves the Co(II)-catalyzed CL of luminol oxidation by H_2O_2 [26]. Luminol solution (0.25 mM, pH 10.8 adjusted with 2 M NaOH) was pumped at 0.10 ml min^{-1} and merged with cobalt nitrate solution (30 μM) flowing at 0.10 ml min^{-1} followed by a mixing coil (0.66 mm × 500 mm), and then the mixed stream reacted with the carrier/sample stream within the lumen of the LCW as the CL signal was collected. Aqueous H_2O_2 standards were prepared by dilution of 30% H_2O_2 (Fisher) and standardized by titration with secondary standard $KMnO_4$. Aqueous H_2O_2 standards with concentration ≤1 mM level were prepared immediately before use to avoid decomposition loss.

All chemicals used were of analytical reagent grade, and freshly deionized water was used throughout all experiments. Excepted as stated, reagents were obtained from Aldrich Chemical and used without further purification.

3. Results and discussion

3.1. Referencing and baseline drift compensation in LPLA measurements

Baseline drifts in LPLA measurements is more common and more significant than with conventional small path length cells. Refractive index effects, that influences absolute light throughput, Schlieren effects and minute gas/air bubbles that tenaciously adhere to a hydrophobic Teflon® AF surface, are the main reasons for baseline shift, drift, and noise. As will be seen below, these can be well compensated by using a nonabsorbing wavelength for reference. The numerical aperture (NA) of an optical fiber depends on the difference of the squares of the refractive indices of the clad and core regions. In this vein, the light throughput in a liquid-filled AF tube is highly dependent on the refractive index of the liquid in the tube. The RI of the AF tube functioning as the "cladding" region of the optical fiber, of course, remains constant. The RI of the solution in the tube is always higher than the RI of the AF tube. Accordingly, the numerical aperture and the light throughput increase dramatically with increasing RI of the inner solution. In flow analysis, it is rarely possible to insure that the RI of the carrier and the injected sample are exactly the same. Therefore, in absorption measurements, if the carrier is water while the sample matrix is an aqueous solution or virtually any other liquid (aqueous solutions that contain dissolved solids or any other liquid has a higher refractive index than water), the measured absorbance will be lower than its true value because there will be an increase in light throughput due to the transient increase in NA. As shown in Fig. 7, the observed absorbance of methyl orange (MO) solution at 475 nm decreases more and more as increasing amounts of nonabsorbing sodium chloride is added to the injected sample, increasing the RI of the sample. In this experiment, the absorbance was measured in a conventional manner, the LED light source being directly referenced on its bottom [4], independent of the measurement cell. In Fig. 8, results of the same experiment is shown but the reference signal in this case is the light

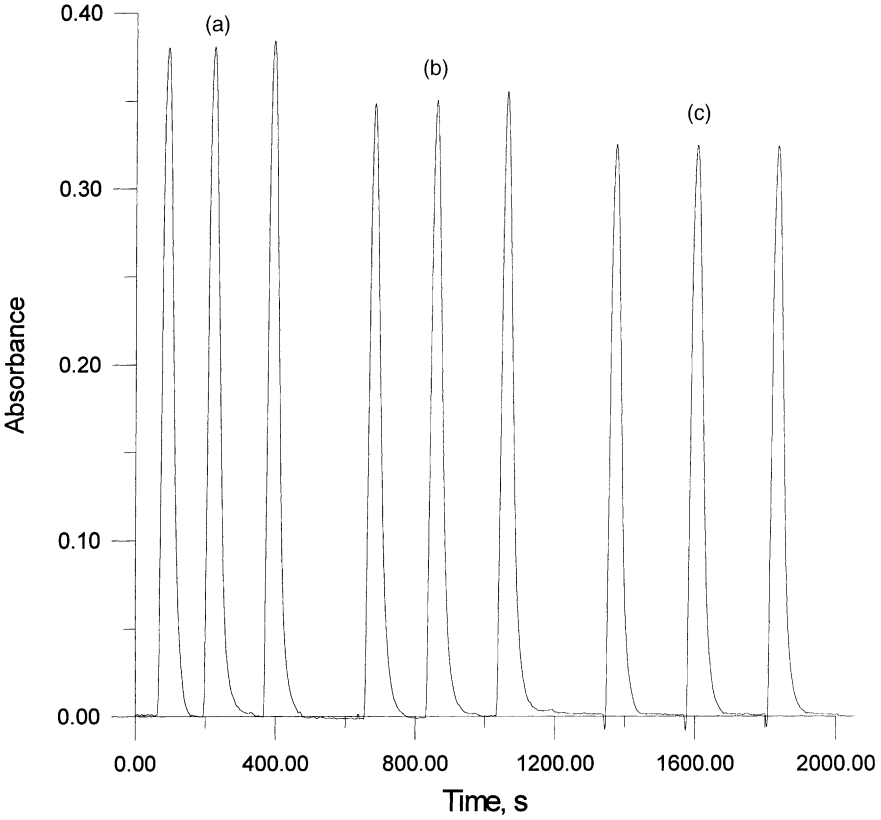

Fig. 7. Response with absorbance detection in the conventional manner, light source referenced independent of measurement cell. Detection wavelength: 475 nm; analyte: methyl orange. (a) Solution in water, (b) solution in 1% (w/v) NaCl, (c) solution in 4% (w/v) NaCl.

intensity passing through the cell at a wavelength of 650 nm; MO does not absorb at this wavelength. The equivalence of all the peak heights in Fig. 8 shows the effectiveness of this referencing technique.

The Schlieren effect caused by a different refractive index front associated with the sample also causes transient shift/noise. In this case, even with conventional cells, it is well known that such artifacts can be drastically reduced by using a second, nonabsorbing wavelength as the reference [37]. The same was observed in the present case and is not further discussed.

As may be imagined, small bubbles (even those invisible to the eye) that enter the cell or adhere to the cell walls also cause baseline shift and noise. Addition of exit restriction to increase backpressure can minimize the occurrence and the size of the bubbles; however, it cannot be eliminated altogether. We show an example of how dramatically bubble induced disturbances can be minimized in Fig. 9. In this experiment, first one and then a consecutive pair of air bubbles were deliberately introduced. The dashed line shows the absorbance signal obtained by conventional referencing of the light source; the solid line is the absorbance signal with a second wavelength as reference. The difference is most remarkable.

3.2. Optimization of S/N obtained with an inexpensive compact CCD spectrometer

3.2.1. Integration time

Table 1 shows the influence of the integration time on the signal to noise ratio when measuring the fluorescence signal of fluorescein with the CCD spectrometer as the detector and LED-4 (λ_{max}: 459 nm) as the excitation source. The S/N increases linearly with

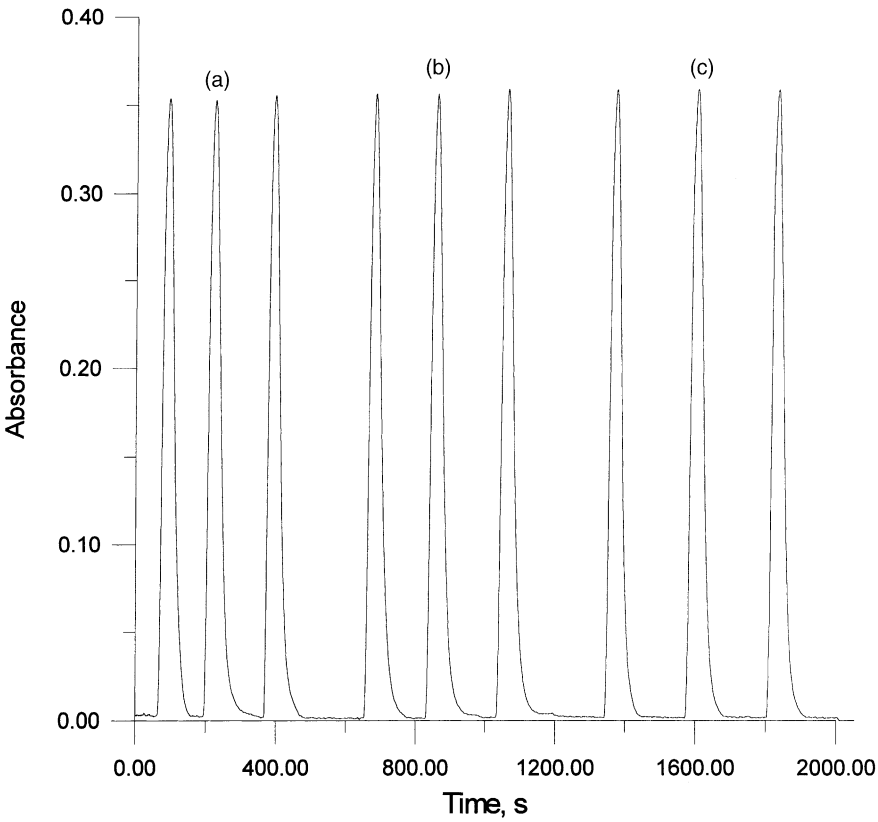

Fig. 8. (a–c) Results of an identical experiment to that in Fig. 7 except that the reference signal was the light intensity through the cell at a wavelength of 650 nm, at which methyl orange does not absorb.

increase of integration time since the noise is nearly independent of the integration time. For absorption measurements, a similar observation is made.

3.2.2. Increasing bandwidth in fluorescence measurements

The wavelength bandwidth for signal measurement is user selectable, from about 7 to 100 nm. Table 2 shows the effects of increasing bandwidth for the measurement of fluorescence signals centered at 520 nm with different bandwidths. The data in Table 2 show that although the S/N increases with the bandwidth at first, it eventually decreases. Although the exact situation will depend on the bandwidth of emission observed with a specific analyte, the gain in S/N by increasing the measurement bandwidth is limited and does not provide a significant S/N advantage. For

Table 1
Influence of integration time

Integration time (ms)	Signal ($n = 3$)	Noise ($n = 3$)	S/N
50	18.8 ± 0.5	0.73 ± 0.01	25.1
200	61.0 ± 0.9	0.74 ± 0.01	82.1
400	117.5 ± 1.2	0.75 ± 0.01	157
800	220.1 ± 2.0	0.81 ± 0.01	270
2000	643.0 ± 4.1	0.94 ± 0.02	684

Table 2
Influence of bandwidth

Bandwidth (nm)	Signal ($n = 3$)	Noise ($n = 3$)	S/N
6.7	220.1 ± 2.0	0.81 ± 0.01	270
16.7	219.7 ± 2.0	0.60 ± 0.01	364
26.7	216.4 ± 2.0	0.49 ± 0.01	441
36.7	210.4 ± 1.9	0.45 ± 0.01	470
66.7	171.4 ± 1.9	0.40 ± 0.004	425
100	133.9 ± 1.8	0.37 ± 0.004	365

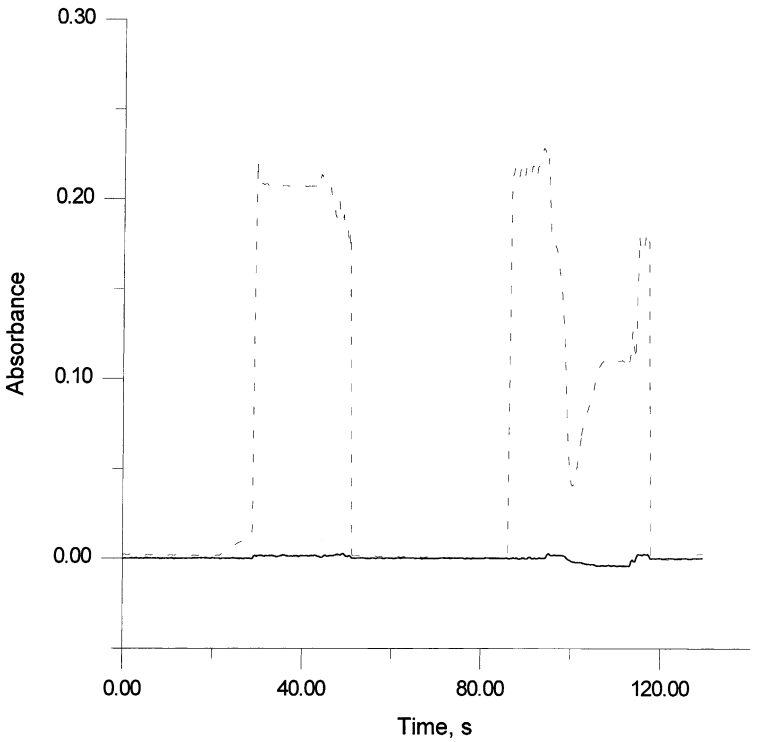

Fig. 9. Influence of a series of air bubbles flowing through the absorbance detector. The dashed line is the absorbance signal with referencing in a conventional manner (light source referenced independently from cell), while the solid line is the absorbance signal with light of a second wavelength passing through the cell as reference.

absorption measurements, the lack of a S/N gain is similar and may be even more apparent.

3.3. Stray light

Light that propagates through the cell walls is essentially stray light and will be collected by the larger diameter larger NA conventional optical fiber placed on the detector side. However, the thin walls of the AF tube (thickness 140 μm), the U-geometry, and the presence of a higher RI medium on the interior side results in virtually no light being conducted through the wall. For absorption measurements, stray light has not therefore been a problem and does not limit adherence to Beer's law only to low absorbance values.

3.4. Analytical performance in LPLA measurements

Solution of several dyes (neutral red (445 nm), brilliant blue (590 nm), and malachite green (620 nm) were first tested. The measured absorbance values were 51.3 ± 0.2 times higher than the respective values for the same solutions measured on a conventional UV-Vis spectrometer (Model 8453A, Agilent), in excellent agreement with the physical AF tube length of 50 cm and possible mismatch in exact wavelength calibration of the two measurement systems.

For the Cr(VI) analysis system, typical system output is shown in Fig. 10 for 0–46.2 $\mu g\,l^{-1}$ Cr(VI). The observed absorbance signal was linear ($r^2 = 0.9999$) with Cr(VI) concentration in the tested range with a slope of 59.5 ± 0.1 mAU per ng Cr(VI). The relative standard deviation at the 46.2 $\mu g\,l^{-1}$ level is 0.4%. In comparison, the use of a conventional 6 mm cell (in a slightly different analytical protocol) led others to a slope of 0.42 mAU ng^{-1} Cr(VI) [38]. The LPLA measurement obviously shows a much better response. Full potential of the technique cannot be realized with the relatively noisy CCD spectrometer used

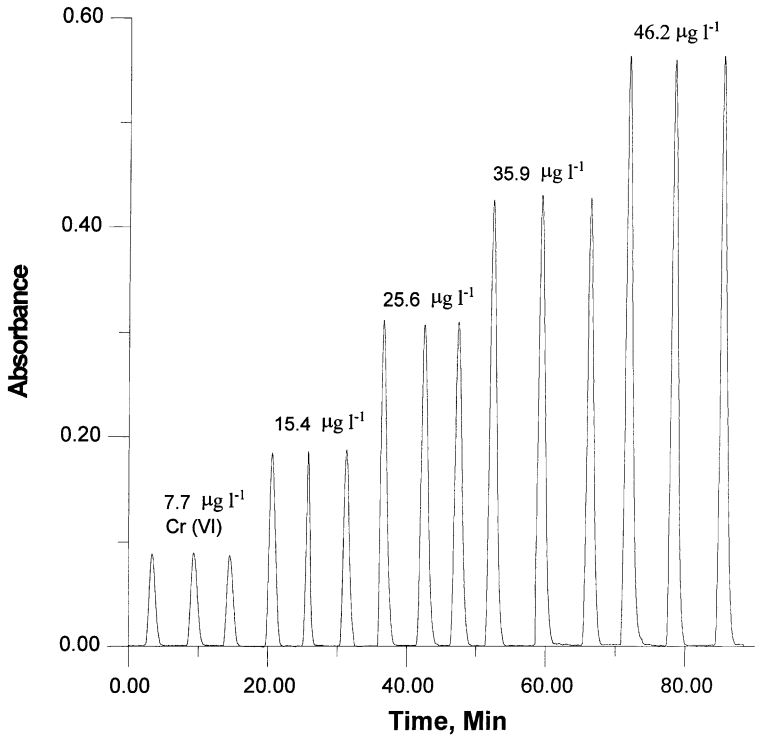

Fig. 10. Typical chart output for determination of chromium(VI).

here, which limits the lowest detectable absorbance to about 0.5 mAU.

For the determination of aluminum in water with PCV [39] by the LPLA method, the absorbance is proportional to the Al concentration in the 0–800 $\mu g\,l^{-1}$ range with a linear $r^2 = 0.9918$ (7 concentration points, $n \geq 3$ at each point) and a slope of 0.84 mAU per $\mu g\,l^{-1}$ Al, the S/N = 3 LOD is calculated to be $5\,\mu g\,l^{-1}$. The relative standard deviation at the $400\,\mu g\,l^{-1}$ level is 1.7% ($n = 5$). For flow-injection analysis with a 10 mm flow-through cell, the response is about 0.35 mAU per $\mu g\,l^{-1}$ Al [39]. A high sensitivity gain cannot be obtained in this case because PCV itself has significant absorbance at the measurement wavelength of 585 nm. As a result, the PCV reagent concentration must be reduced to less than the optimum (the concentration at which added Al is fully complexed [39] to get enough light output after absorption. The concentration of PCV used in the LPLA experiment (0.1 mM) is 100 times lower than the recommended value [39]. Obviously, the complexation constant between Al(III) and PCV is not large enough to permit near quantitative formation of the colored Al chelate. This decrease of the colored Al chelate with decreasing PCV concentration results in a relative decrease of sensitivity. However, if the complexation constant were large enough, there would have been no loss of sensitivity. In such a situation, the LPLA method will still have an obvious sensitivity advantage. In general, LPLA methods will provide a good sensitivity gain only in those methods where the background absorbance is low.

3.5. *Performance for fluorescence measurements with CCD spectrometer*

In applications where the ultimate in sensitivity is not required, the CCD spectrometer suffices and allows the collection of the entire fluorescence spectra. The excitation LED that gives the maximum emission must be first chosen. In much the same way a conventional fluorescence spectrometer performs an excitation scan, the elements of the LED excitation array are turned on one by one, thus generating a series

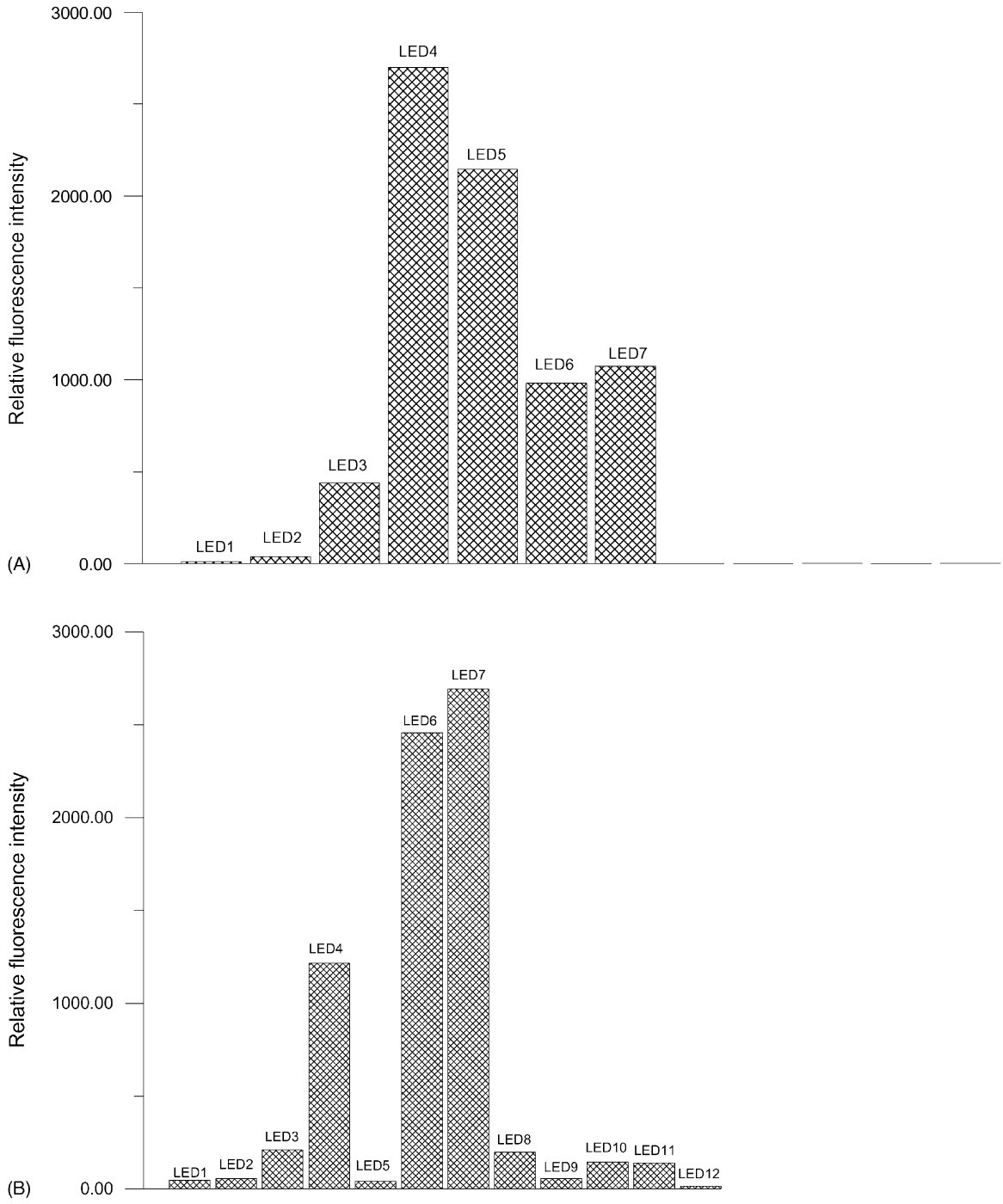

Fig. 11. Excitation “spectra” for (A) fluorescein (emission at 535 nm), (B) Rhodamine B (emission at 585 nm).

of excitation spectra, the totality of which represents the conventional excitation spectra. While a 3D plot can be generated from these data, since the emission peak remains in the same place, the peak intensity at this wavelength can be plotted as a representation of the excitation spectra. As shown in Fig. 2, the light intensity of individual LEDs in the excitation array varies greatly, and unless corrected for, the excitation spectrum thus obtained will be different in quantitative details from one generated by a conventional fluorescence spectrometer. Nevertheless, excitation spectra for different analytes as obtained in the present instrument can be just as dramatically different as in a conventional spectrofluorometer. Fig. 11 shows the excitation spectra of fluorescein and Rhodamine B as obtained with the present instrument.

The detection performance of the CCD spectrometer is exemplified by the LOD (S/N = 3) of fluorescein being 0.53 nM with an integration time of 2 s and LED-4 (λ_{max}: 459 nm) as excitation source. For calcein blue, which displays a lower quantum efficiency and excited by a lower power emitter (LED-1, λ_{max}: 375 nm), the LOD was 31 nM with an integration time of 4 s.

3.6. Fluorescence detection capabilities with miniature PMT

For the determination of aqueous H_2O_2, in the tested range of 0–10 μM, the fluorescence intensity is linear with the hydrogen peroxide concentration with r^2 of 0.9983. The relative standard deviation at the 10 μM analyte level was 0.93%. The S/N = 3 LOD was 16 nM. In contrast, when the CCD spectrometer is used as detector, the LOD (S/N = 3) is only 51 μM with an integration time of 2 s. For the determination of gaseous H_2O_2, the typical system output for 0–5 ppbv (10^{-9} atm) H_2O_2 is shown in Fig. 12. The fluorescence signal is proportional to the hydrogen peroxide concentration with r^2 of 0.9937. The relative

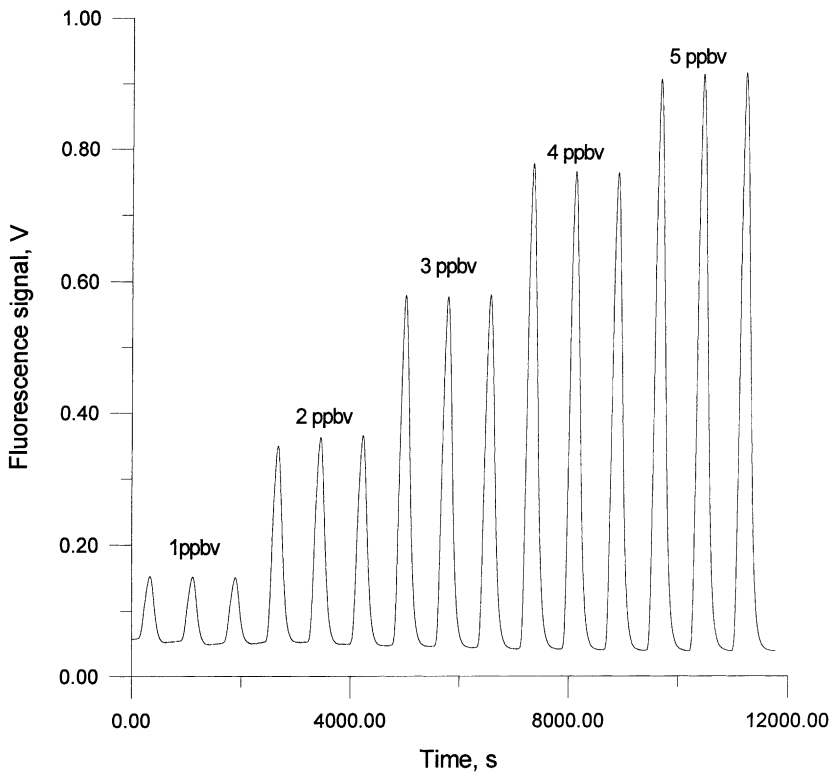

Fig. 12. Typical chart out put for determination of gaseous H_2O_2.

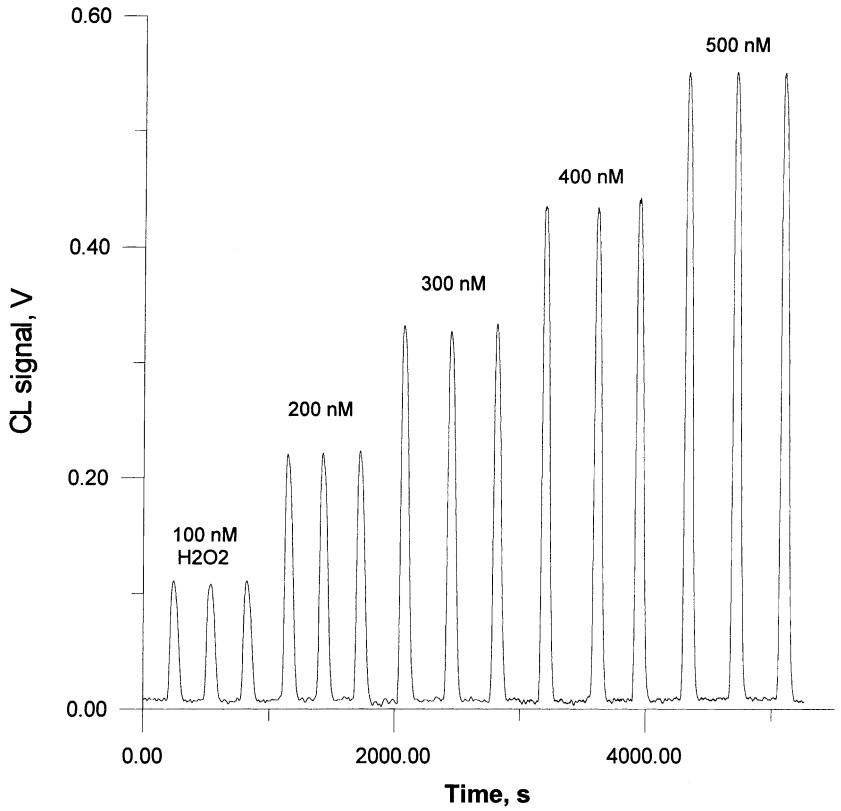

Fig. 13. Typical chart out put for determination of aqueous H_2O_2.

standard deviation at the 5 ppbv level was 0.57%. The S/N = 3 LOD was calculated to be 8.0 pptv, actually better than the LOD of 13.5 pptv reported for a dedicated instrument [21].

3.7. Performance for chemiluminescence measurements

Typical system output for the determination of aqueous H_2O_2 is shown in Fig. 13. The peak height of the CL signal is linear with the H_2O_2 concentration with an r^2 of 0.9991 in the range of 0–500 nM. The relative standard deviation at the 500 nM level is 1.4% ($n = 7$). The S/N = 3 LOD is calculated to be 4.0 nM. With a gas diffusion scrubber as used in the determination of H_2O_2 by the fluorescence method, the observed LOD for measuring gaseous H_2O_2 was found to be 16 pptv, adequate for all ambient atmospheric measurement applications.

4. Conclusions

We have described here a versatile simple, inexpensive and portable flow analyzer that is applicable to a variety of different types of measurements, capable of high sensitivity and applicable to a wide range of analytes. The long path length absorbance detector provides can provide 50 times better sensitivity than a conventional 1 cm cell; however, this sensitivity gain cannot be realized for high background absorbance methods. The transverse illumination fluorescence detector using a solid-state excitation source array provides a simple and novel approach to spectrofluorometric measurements. The chemiluminescence detector, in which the LCW works as both mixing coil and light collector, provides sensitive and highly reproducible measurements. Switching from one detection mode to another is straightforward and rapid. It is thus an ideal instrument not only for developing and

checking the performance of new analytical methods in more than one detection mode, it is also a practical instrument for doing trace analysis in the field.

Acknowledgements

IMRJ would like to express his gratitude to the American Chemical Society (ACS) and the Brazilian Chemical Society for the support of an ACS fellowship within the aegis of an intersociety cooperative program that made possible his participation in this work. Work done at Texas Tech was supported by DARPA under a program monitored by Dr. J. Carrano. We also thank SBC COM for partial support. We thank an anonymous reviewer for significant improvements of this paper.

References

[1] J. Ruzicka, E.H. Hansen, Anal. Chim. Acta 78 (1975) 145.
[2] J. Ruzicka, G.D. Marshall, Anal. Chim. Acta 237 (1990) 329.
[3] W. Baumann, Fresenius Z. Anal. Chem. 284 (1977) 31.
[4] P.K. Dasgupta, H.S. Bellamy, H. Liu, J.L. Lopez, E.L. Loree, K. Morris, K. Petersen, K.A. Mir, Talanta 40 (1993) 53.
[5] P. Dress, H. Franke, Appl. Phys. B: Laser Opt. 63 (1996) 12.
[6] P. Dress, H. Franke, Proc. SPIE 2686 (1996) 157.
[7] R.D. Waterbury, W. Yao, R.H. Byrne, Anal. Chim. Acta 357 (1997) 99.
[8] R. Altkorn, I. Koev, A. Gottlieb, Appl. Spectrosc. 51 (1997) 1554.
[9] P. DeLand, American Laboratory, November 1997, p. 12.
[10] P.K. Dasgupta, Z. Genfa, S.K. Poruthoor, S. Caldwell, S. Dong, S.-Y. Liu, Anal. Chem. 70 (1998) 4661.
[11] P. Dress, M. Belz, K.F. Klein, K.T.V. Grattan, H. Franke, Appl. Opt. 37 (1998) 4991.
[12] M. Belz, P. Dress, K.F. Klein, W.J.O. Boyle, H. Franke, K.T.V. Grattan, Water Sci. Technol. 37 (1998) 279.
[13] C. Gooijer, G. Hoornweg, T.D. Beer, A. Bader, D.J. Iperen, U.A. Brinkman, J. Chromatogr. A 824 (1998) 1.
[14] W. Yao, R.H. Byrne, R.D. Waterbury, Environ. Sci. Technol. 32 (1998) 2646.
[15] W. Yao, R.H. Byrne, Talanta 48 (1999) 277.
[16] S. Jambunathan, P.K. Dasgupta, J. Soc. Leather Technol. Chem. 84 (2000) 63.
[17] M.R. Milani, P.K. Dasgupta, Anal. Chim. Acta 431 (2001) 169.
[18] P.K. Dasgupta, Z. Genfa, J. Li, C.B. Boring, S. Jambunathan, R. Al-Horr, Anal. Chem. 71 (1999) 1400.
[19] J. Li, P.K. Dasgupta, Z. Genfa, Talanta 50 (1999) 617.
[20] R.H. Byrne, W. Yao, E. Kaltenbacher, R.D. Waterbury, Talanta 50 (2000) 1307.
[21] J. Li, P.K. Dasgupta, Anal. Chem. 72 (2000) 5338.
[22] J. Li, P.K. Dasgupta, Z. Genfa, M.A. Hutterli, Field Anal. Chem. Technol. 5 (2001) 2.
[23] S.L. Wang, X.J. Huang, Z.L. Fang, P.K. Dasgupta, Anal. Chem. 73 (2001) 4545.
[24] P.K. Dasgupta, US Patent 6,332,049 Luminescence Detector with Liquid Core Waveguide (18 December 2001).
[25] J. Li, P.K. Dasgupta, Anal. Chim. Acta 398 (1999) 33.
[26] J. Li, P.K. Dasgupta, Anal. Chim. Acta 442 (2001) 63.
[27] http://www.globalfia.com/whatsnew/firefly.html.
[28] V. Kuryatkov, B. Borisov, S. Nikishin, M. Holtz, S.N.G. Chu, H. Temkin, Phys. Stat. Sol. A 192 (2002) 286–291.
[29] http://www.scientificsonline.com/ec/products/display.cfm?categoryid=192886.
[30] P.K. Dasgupta, in: J. Pawliszyn (Ed.), Sampling and Sample Preparation Techniques for Field and Laboratory, vol. XXXVII, Wilson and Wilson's Comprehensive Analytical Chemistry Series, Elsevier, Amsterdam, 2002, pp. 97–160.
[31] A. Moulin, Bull. Chem. Soc. Paris 31 (1904) 295.
[32] Standard Test Methods for Chromium in Water, Method D 1687–1992, Annual Book of Standards, Part 11, ASTM Committee D19, American Society for Testing of Materials, Washington, DC, 1992, p. 492.
[33] M.D. Cohen, J.T. Zelikoff, L.C. Chen, R.B. Schlesinger, Inhal. Toxicol. 9 (1997) 834.
[34] A.I. Vogel, A Textbook of Qualitative Inorganic Analysis, fourth ed., Longmans Green, London, 1954, p. 210.
[35] A. Anton, Anal. Chem. 32 (1960) 725.
[36] B.F. Reis, H. Bergamin, E.A.G. Zagatto, F.J. Krug, Anal. Chim. Acta 107 (1979) 309.
[37] H. Liu, P.K. Dasgupta, Anal. Chim. Acta 289 (1994) 347.
[38] G. Samanta, C.B. Boring, P.K. Dasgupta, Anal. Chem. 73 (2001) 2034.
[39] O. Royset, Anal. Chim. Acta 185 (1986) 75.